Reappraisal of constraints on Z' models from unitarity and direct searches at the LHC

Triparno Bandyopadhyay,[1,*] Gautam Bhattacharyya,[2,†] Dipankar Das,[1,‡] and Amitava Raychaudhuri[1,§]

[1]*Department of Physics, University of Calcutta, 92 Acharya Prafulla Chandra Road, Kolkata 700009, India*
[2]*Saha Institute of Nuclear Physics, HBNI, 1/AF Bidhan Nagar, Kolkata 700064, India*

In a truly model-independent approach, we reexamine a minimal extension of the Standard Model (SM) through the introduction of an additional $U(1)$ symmetry leading to a new neutral gauge boson (Z'), allowing its kinetic mixing with the hypercharge gauge boson. An SM neutral scalar is used to spontaneously break this extra symmetry, leading to the mass of the Z'. Except for three right-handed neutrinos, no other fermions are added. We use the current LHC Drell-Yan data to put model-independent constraints in the parameter space of three quantities, namely, $M_{Z'}$, the Z-Z' mixing angle (α_z), and the extra $U(1)$ effective gauge coupling (g'_x), which absorb all model dependence. We impose additional constraints from unitarity and low-energy neutrino-electron scattering. However, limits extracted from direct searches turn out to be most stringent. We obtain $M_{Z'} > 4.4$ TeV and $|\alpha_z| < 0.001$ at 95% C.L., when the strength of the additional $U(1)$ gauge coupling is the same as that of the SM $SU(2)_L$.

I. INTRODUCTION

Of all the beyond–Standard Model (BSM) scenarios, none is more ubiquitous than models with an extra $U(1)$ symmetry in addition to the Standard Model (SM) symmetry, giving a neutral spin-1 massive gauge boson, Z'. Its theoretical motivation comes from various directions. Left-right symmetric models, grand unified theories (GUTs) larger than $SU(5)$, e.g., $SO(10)$ or E_6, as well as string models, all entail an extra gauged $U(1)$ in addition to the SM group [1–14]. Nonsupersymmetric BSM scenarios, advocated to address the hierarchy problem, such as little Higgs models [15,16] with extended gauge sectors, contain $U(1)$ as an extra gauge group. Even dynamical supersymmetry breaking triggered by an anomalous $U(1)$ has been extensively discussed (for a review, see Ref. [17]). Leaking of the standard Z boson into an extra dimension yields, from a four-dimensional perspective, an infinite tower of increasingly more massive Kaluza-Klein modes, each such mode resembling a Z' boson of a gauged $U(1)$ carrying

specific symmetries [18–20]. Besides, a Z' model with a gauged $(B − L)$ symmetry has been used to address the hierarchy problem by facilitating electroweak symmetry breaking radiatively *à la* Coleman-Weinberg keeping classical conformal invariance and stability up to the Planck scale [21]. Cosmological inflation scenarios with nonminimal gravitational coupling have been studied in a similar context in which the inflaton coupling is correlated to the Z' coupling [22]. $U(1)$ gauge bosons also constitute important ingredients in cosmic string models [23].

On the other hand, Z' has been fruitfully employed in many theoretically well-motivated models as a portal to dark matter (DM), mediating between the dark sector and the visible sector [24–30]. The DM itself could be a $U(1)$ gauge boson of the dark sector. A heavy Z' in such models could be realized in a gauge-invariant way by the Stückelberg mechanism [31]. In the astrophysical context, too, a Z' gauge boson has been advocated to account for the γ-ray excess in the Galactic center [32,33].

Thus, there is enough motivation for the Z' mass and coupling to be an important part of phenomenological studies in the context of colliders [10,34–39], the collider–dark matter interface [40–44], flavor physics [45,46], and electroweak precision tests [47–49]. In this work, we use the latest ATLAS (LHC) Drell-Yan (DY) data (36 fb⁻¹ luminosity) to set model-independent bounds on the fermionic couplings of Z'. For this, we use the data for both (e^+e^-, $\mu^+\mu^-$) as well as the $\tau^+\tau^-$ final states. In addition, we use s-wave unitarity to set upper bounds on $M_{Z'}$ as a function of the Z-Z' mixing angle (α_z).

*gondogolegogol@gmail.com
†ddphy@caluniv.ac.in
‡gautam.bhattacharyya@saha.ac.in
§palitprof@gmail.com

Additionally, we use the low-energy ν_μ-e scattering data to constrain the Z' parameter space. The LHC DY data turn out to be most constraining compared to the other two considerations. This does not undermine the relevance of the other two constraints, which have situational merits. The unitarity bound holds, irrespective of the Z' coupling to fermions, whereas the ν_μ-e scattering limits become important for hadrophobic Z's. Taking into account all the bounds, we obtain strong constraints in the complete parameter space spanned by only three independent parameters: $M_{Z'}$, α_z, and g'_x, the effective gauge coupling of the additional $U(1)$ taking into account the scope for kinetic mixing. We make an important observation that all model dependence can be absorbed within the above three parameters as long as the additional $U(1)$ is nonanomalous.

Very recently, constraints directly on $M_{Z'}$ for various $U(1)$ extensions were derived in Ref. [50] using the 36 fb^{-1} ATLAS data, and wherever we overlap, we roughly agree with their limits. Constraints directly on $M_{Z'}$ were also obtained in Ref. [51] assuming that the Z-Z' mixing angle is small, but those limits are obviously a bit weaker as they were extracted using the then-available ATLAS data with much lower luminosity.

Our paper is organized as follows. In Sec. II, we set up our notations recapitulating the Z' extension of the SM, touching upon the scalar and the fermion sectors. Then, in Sec. III, we use the latest 36 fb^{-1} ATLAS DY data [52,53] to set constraints on its fermionic couplings for different Z' masses in a model-independent manner. Next, in Sec. IV, we discuss the bounds on the Z' mass and the Z-Z' mixing angle arising from s-wave unitarity. Note that this bound depends only on $M_{Z'}$ and the Z-Z' mixing angle and is independent of the Z' couplings to the fermions. Once those fermionic couplings are chosen, a bound on the same plane arises from the low-energy ν_μ-e scattering data, which we discuss in Sec. V. In Sec. VI, we combine the limits arising from these aspects to identify the region currently allowed for different $U(1)$ extensions. We end with our conclusions, in which we highlight the new features arising out of our analysis.

II. MINIMAL Z' MODEL—A SMALL RECAPITULATION

As noted in the Introduction, BSM scenarios with an electrically neutral, massive vector boson, Z', are quite common in the literature. The simplest realizations of Z' models are the ones in which the SM gauge symmetry, $\mathcal{G}_{SM} \equiv SU(3)_C \otimes SU(2)_L \otimes U(1)_Y$, is minimally extended to $\mathcal{G}_{SM} \otimes U(1)_X$. The $U(1)_X$ is broken by a $\mathcal{G}_{SM}$ singlet scalar, S, charged under $U(1)_X$. Without any loss of generality, we choose this charge to be $1/2$, which fixes the convention for g_x—the gauge coupling corresponding to $U(1)_X$. Thus, in the minimalistic scenario, we have the scalar multiplets, transforming under $SU(3)_C \times SU(2)_L \times U(1)_Y \times U(1)_X$ as

$$\Phi \equiv (1, 2, 1/2, x_\Phi/2); \qquad S \equiv (1, 1, 0, 1/2), \quad (1)$$

where Φ denotes the usual $SU(2)_L$ doublet responsible for the SM gauge symmetry breaking as well as the Dirac masses of fermions. The quantities inside the parentheses characterize the transformation properties under the gauge group $SU(3)_C \otimes SU(2)_L \otimes U(1)_Y \otimes U(1)_X$. The electric charge is given by

$$Q = T_{3L} + Y, \quad (2)$$

where T_{3L} and Y are the third component of weak isospin and the hypercharge, respectively. As Φ transforms in a nontrivial fashion under $SU(2)_L$, $U(1)_Y$, and $U(1)_X$, there will be mixing among the neutral gauge boson states when Φ develops a vacuum expectation value (vev). The mass eigenstates that emerge will be identified as the massless photon (A), the SM Z, and an exotic Z'. Note that, even if we start with $x_\Phi = 0$, Φ can develop a $U(1)_X$ charge due to gauge-kinetic mixing among the two Abelian field strength tensors [54]. Also, in general, there will be mixing among the neutral scalars coming from Φ and S, and a certain composition of the two should correspond to the SM-like scalar observed at the LHC.

Abelian extensions of the SM are typically motivated by some high-scale physics related to an elaborate scalar sector, and it might seem that the two-scalar scenario we are considering here is a bit too simplistic. However, we are interested in models in which the new physics beyond the extra $U(1)_X$ is at too high a scale to have any meaningful contribution to $\mathcal{O}(\text{TeV})$ physics, or too weakly coupled. With that in mind, such a minimal framework is capable of describing the gauge-scalar sector of a wide array of $U(1)$ extensions of the SM, which are differentiated by the fermionic charges under the $U(1)_X$. In the following subsections, we describe our framework in detail. In passing, it should be noted that in the literature one is often faced with models in which the extended gauge symmetry is given by $SU(3)_C \otimes SU(2)_L \otimes U(1)_1 \otimes U(1)_2$, where the SM $U(1)_Y$ is a linear combination of $U(1)_1$ and $U(1)_2$. An example is $U(1)_R \otimes U(1)_{B-L}$, of left-right symmetric models. In such cases, we can readily perform a rotation among the $U(1)$ generators to obtain the $U(1)_Y \otimes U(1)_X$ basis that we are using.

A. Gauge-scalar sector

The gauge-scalar part of the Lagrangian for minimal $\mathcal{G}_{SM} \otimes U(1)_X$ models is given by

$$\mathcal{L} = \mathcal{L}_{GK} + \mathcal{L}_{SK} - V(\Phi, S), \quad (3)$$

where $\mathcal{L}_{GK}$ and $\mathcal{L}_{SK}$ are the kinetic Lagrangians in the gauge and the scalar sectors, respectively, and $V(\Phi, S)$ denotes the scalar potential, expressions for which appear below:

$$\mathcal{L}_{\mathrm{GK}} = -\frac{1}{4} W^a_{\mu\nu} W^{\mu\nu}_a - \frac{1}{4} B_{\mu\nu} B^{\mu\nu} - \frac{1}{4} X_{\mu\nu} X^{\mu\nu}$$
$$- \frac{\sin\chi}{2} B_{\mu\nu} X^{\mu\nu}, \tag{4a}$$

$$\mathcal{L}_{\mathrm{SK}} = (D^\mu \Phi)^\dagger (D_\mu \Phi) + (D^\mu S)^\dagger (D_\mu S), \tag{4b}$$

$$V(\Phi, S) = -\mu^2 (\Phi^\dagger \Phi) - \mu_S^2 (S^\dagger S) + \lambda_\Phi (\Phi^\dagger \Phi)^2$$
$$+ \lambda_S (S^\dagger S)^2 + \lambda_{\Phi S} (\Phi^\dagger \Phi)(S^\dagger S). \tag{4c}$$

Above, $W^a_{\mu\nu}$, $B_{\mu\nu}$, and $X_{\mu\nu}$ denote the field tensors corresponding to $SU(2)_L$, $U(1)_Y$, and $U(1)_X$ respectively, and the covariant derivatives for Φ and S are given by

$$D_\mu \Phi = \left(\partial_\mu - ig\frac{\tau_a}{2} W^a_\mu - i\frac{g_Y}{2} B_\mu - i\frac{g_x}{2} x_\Phi X_\mu \right) \Phi, \tag{5a}$$

$$D_\mu S = \left(\partial_\mu - i\frac{g_x}{2} X_\mu \right) S, \tag{5b}$$

where τ_a represents the Pauli matrices and the naming convention of the gauge fields mirrors that of the field strength tensors.

Note that, in the $(B^{\mu\nu}, X^{\mu\nu})$ basis, $\mathcal{L}_{\mathrm{GK}}$ contains the gauge kinetic mixing term $(\sin\chi/2) B_{\mu\nu} X^{\mu\nu}$ [54]. Such a term should, in general, be present in the Lagrangian as it is both Lorentz and gauge invariant. In a UV-complete theory, the parameter χ should be calculable by integrating out heavy states at the appropriate scale. However, we stay blind to such UV completion and treat χ as a general parameter. We can perform a general linear transformation to go to a basis in which $\mathcal{L}_{\mathrm{GK}}$ is canonically diagonal [55,56]:

$$\begin{pmatrix} B_\mu \\ X_\mu \end{pmatrix} \to \begin{pmatrix} B'_\mu \\ X'_\mu \end{pmatrix} = \begin{pmatrix} 1 & \sin\chi \\ 0 & \cos\chi \end{pmatrix} \begin{pmatrix} B_\mu \\ X_\mu \end{pmatrix}. \tag{6}$$

In this basis, the gauge-kinetic Lagrangian becomes

$$\mathcal{L}_{\mathrm{GK}} = -\frac{1}{4} W^a_{\mu\nu} W^{\mu\nu}_a - \frac{1}{4} B'_{\mu\nu} B'^{\mu\nu} - \frac{1}{4} X'_{\mu\nu} X'^{\mu\nu}, \tag{7}$$

and the covariant derivatives take the forms

$$D_\mu \Phi = \partial_\mu \Phi - i\frac{g}{2} (\tau_a W^a_\mu + \tan\theta_w B'_\mu + \tan\theta_x x'_\Phi X'_\mu) \Phi, \tag{8a}$$

$$D_\mu S = \left(\partial_\mu - i\frac{g'_x}{2} X'_\mu \right) S, \tag{8b}$$

where we have defined

$$\tan\theta_w = \frac{g_Y}{g}, \tag{9a}$$

$$\tan\theta_x = \frac{g'_x}{g}, \tag{9b}$$

with $\quad g'_x = g_x \sec\chi,$ (9c)

and $\quad x'_\Phi = x_\Phi - \frac{g_Y}{g_x} \sin\chi.$ (9d)

Equations (9c) and (9d) reflect how the definitions of the gauge coupling and the gauge charge of Φ corresponding to the extra $U(1)$ will be modified in the presence of kinetic mixing. In the limit of zero kinetic mixing, $\tan\theta_x$ characterizes the strength of the $U(1)_X$ gauge coupling relative to the weak gauge coupling.

After spontaneous symmetry breaking, we expand the scalar fields, in the unitary gauge, as

$$\Phi = \frac{1}{\sqrt{2}} \begin{pmatrix} 0 \\ v + \phi_0 \end{pmatrix}, \qquad S = \frac{1}{\sqrt{2}} (v_s + s), \tag{10}$$

where v and v_s are the vevs for Φ and S, respectively. This will lead to the neutral gauge boson mass matrix, in the basis in which the gauge kinetic terms are diagonal, which can be written as

$$\mathcal{L}_N^{\mathrm{mass}} = \frac{1}{2} \begin{pmatrix} W^3_\mu & B'_\mu & X'_\mu \end{pmatrix} \cdot \mathcal{M}_N^2 \cdot \begin{pmatrix} W^3_\mu \\ B'_\mu \\ X'_\mu \end{pmatrix}, \tag{11}$$

where

$$\mathcal{M}_N^2 = \frac{g^2 v^2}{4} \begin{pmatrix} 1 & -\tan\theta_w & -x'_\Phi \tan\theta_x \\ -\tan\theta_w & \tan^2\theta_w & x'_\Phi \tan\theta_x \tan\theta_w \\ -x'_\Phi \tan\theta_x & x'_\Phi \tan\theta_x \tan\theta_w & \tan^2\theta_x (r^2 + x'^2_\Phi) \end{pmatrix}, \tag{12}$$

with $r = v_s/v$. The mass matrix in Eq. (12) can be block diagonalized as

$$O_w^T \cdot \mathcal{M}_N^2 \cdot O_w = \frac{g^2 v^2}{4} \begin{pmatrix} 0 & 0 & 0 \\ 0 & \sec^2\theta_w & -x'_\Phi \tan\theta_x \sec\theta_w \\ 0 & -x'_\Phi \tan\theta_x \sec\theta_w & \tan^2\theta_x (r^2 + x'^2_\Phi) \end{pmatrix}, \tag{13}$$

where

$$O_w = \begin{pmatrix} \sin\theta_w & \cos\theta_w & 0 \\ \cos\theta_w & -\sin\theta_w & 0 \\ 0 & 0 & 1 \end{pmatrix}. \tag{14}$$

The massless photon, A_μ, is then readily extracted as

$$\begin{pmatrix} A_\mu \\ Z_{1\mu} \\ X'_\mu \end{pmatrix} = O_w^T \begin{pmatrix} W^3_\mu \\ B'_\mu \\ X'_\mu \end{pmatrix}. \tag{15}$$

Diagonalization of the remaining 2×2 block of the matrix in Eq. (13) gives rise to the remaining mass eigenstates, namely, Z and Z'. The rotation between the gauge and the mass bases is given by

$$\begin{pmatrix} B'_\mu \\ W^3_\mu \\ X'_\mu \end{pmatrix} = \begin{pmatrix} \cos\theta_w & -\sin\theta_w \cos\alpha_z & \sin\theta_w \sin\alpha_z \\ \sin\theta_w & \cos\theta_w \cos\alpha_z & -\cos\theta_w \sin\alpha_z \\ 0 & \sin\alpha_z & \cos\alpha_z \end{pmatrix} \begin{pmatrix} A_\mu \\ Z_\mu \\ Z'_\mu \end{pmatrix}. \tag{16}$$

This second step of diagonalization then entails the relations

$$M_{11}^2 \equiv M_Z^2 \cos^2\alpha_z + M_{Z'}^2 \sin^2\alpha_z = \frac{M_W^2}{\cos^2\theta_w}, \tag{17a}$$

$$M_{Z'}^2 \cos^2\alpha_z + M_Z^2 \sin^2\alpha_z = M_W^2 \tan^2\theta_x (r^2 + x_\Phi'^2), \tag{17b}$$

$$(M_{Z'}^2 - M_Z^2)\sin 2\alpha_z = \frac{2x_\Phi' \tan\theta_x M_W^2}{\cos\theta_w}, \tag{17c}$$

where $M_W = gv/2$ denotes the W-boson mass. We use Eq. (17) to replace θ_w, r, and x_Φ' in terms of $M_{Z'}$, α_z, and $\tan\theta_x$. As we will see later, the latter three quantities can be extracted directly from data in a model-independent way. It is important to note that we have not treated θ_w as the conventional weak (Weinberg) angle under the implicit *a priori* assumption that α_z is small; rather, we traded it in favor of $M_{Z'}$ and α_z using Eq. (17a). While the gauge-scalar sector described here holds generally for minimal Z' models, the fermion charge assignments vary across them. However, a general formalism can be developed for the fermionic sector as well, which we discuss in the next subsection.

B. Anomaly cancellation and fermionic charge assignments

In this work, we look at the models in which the fermion sector of the SM is extended by a right-handed (RH) neutrino, N_R, per generation. We are interested in the situation in which the RH neutrinos get Majorana masses from their Yukawa interactions with S. Under the assumption of generation universality, the possible $U(1)_X$ charge options for the fermions are quite restricted, as we now discuss.

We assign a $U(1)_X$ charge x_q for the left-handed quark doublets and x_l for the left-handed lepton doublets. For the right-handed u-type (d-type) quarks, we assign the charges x_u (x_d), while for the right-handed electron, we take it to be x_e. The $U(1)_X$ charge of the right-handed neutrinos, N, is taken as x_N. The $U(1)_X$ quantum numbers of the scalars have already been introduced: the SM Higgs doublet, Φ, has a charge $x_\Phi/2$, while S has a charge $1/2$.

Since the scalar Φ is responsible for the fermion Dirac masses, we must have

$$x_q - x_u = x_e - x_l = x_d - x_q = -\frac{x_\Phi}{2}. \tag{18}$$

In addition, since S is assumed to be responsible for the Majorana masses of the right-handed neutrinos, x_N can be determined as

$$x_N = -1/4. \tag{19}$$

Further, demanding cancellation of gauge and gravitational anomalies, we get

$$[SU(2)_L]^2 U(1)_X \Rightarrow 3x_q + x_l = 0, \tag{20a}$$

$$[SU(3)_C]^2 U(1)_X \Rightarrow 2x_q = x_d + x_u, \tag{20b}$$

$$[U(1)_Y]^2 U(1)_X \Rightarrow 2x_q + 6x_l = 16x_u + 4x_d + 12x_e, \tag{20c}$$

$$\text{Gauge Gravity} \Rightarrow 6x_q + 2x_l = 3(x_u + x_d) + (x_e + x_N). \tag{20d}$$

It can be checked that the other two constraints that follow from the $U(1)_Y[U(1)_X]^2$ and $[U(1)_X]^3$ triangle anomalies are automatically satisfied. Equation (20) contains four relations among the six unknowns x_q, x_l, x_u, x_d, x_e, and x_N. Taken together with Eq. (18) and bearing in mind that x_N is fixed from Eq. (19), all the $U(1)_X$ charges of the fermions can be determined in terms of one free parameter,[1] κ_x, as depicted in Table I.

Different $U(1)_X$ models are obtained by choosing κ_x appropriately. In Table II, we have shown several alternatives. For example, the $(B - L)$ extension of the SM corresponds to $\kappa_x = 1/4$. For this choice, the x charges are precisely $(B - L)/4$—the overall factor of $1/4$ being a reflection of our chosen normalization of the $U(1)_X$ coupling constant, g_x. It is worth noting that for this choice of κ_x the $SU(2)_L$ doublet scalar Φ has $U(1)_X$ charge $x_\Phi/2 = 0$. Hence, the Z-Z' mixing in $B - L$ models is strictly due to gauge kinetic mixing, which imparts a $U(1)_X$ charge onto Φ. The choice $\kappa_x = 0$ corresponds to the case in which $U(1)_X \equiv U(1)_R$ under which the left-handed fermions are singlets while right-handed fermions have charges $\pm 1/4$. The choice $\kappa_x = 3/20$ gives $U(1)_X \equiv U(1)_\chi$, which emerges when an $SO(10)$ GUT is broken to $SU(5) \times U(1)_\chi$. Finally, with $\kappa_x = 1/5$, we get the $U(1)_R \times U(1)_{B-L}$ model, which can be rotated to the $U(1)_Y \times U(1)_X$ form

---

[1]Reference [51] also introduces a parametrization for the Z' fermionic charges, but our formulation is slightly different.

TABLE I.   The $U(1)_X$-charge assignments of the multiplets, as a function of κ_x, satisfying the anomaly constraints, as well as the transformation properties of the multiplets under the SM part of the gauge symmetry.

Multiplet	$SU(3)_C$	$SU(2)_L$	$U(1)_Y$	$U(1)_X$
Q_L	3	2	1/6	$\kappa_x/3$
u_R	3	1	2/3	$4\kappa_x/3 - 1/4$
d_R	3	1	−1/3	$-2\kappa_x/3 + 1/4$
L_L	1	2	−1/2	$-\kappa_x$
e_R	1	1	−1	$-2\kappa_x + 1/4$
N_R	1	1	0	−1/4
Φ	1	2	1/2	$\kappa_x - 1/4$
S	1	1	0	1/2

with the $U(1)_X$ charge satisfying $5x = (B - L) - T_{3R}/2$. In Table II, we have also summarized how the usually normalized $U(1)$ charges in these models are related to the $U(1)_X$ charges given in the last column of Table I.

C. Fermion couplings to gauge bosons

The parametrization for fermion charges being set, we can now write down the fermion couplings to Z and Z', which will be necessary for the subsequent discussions. The relevant interaction Lagrangian can be written as

$$\mathcal{L}_{\text{int}} = -\frac{g}{2\cos\theta_w}[\bar{f}\gamma^\mu(g_V^f - g_A^f\gamma^5)fZ_\mu + \bar{f}\gamma^\mu(g_V'^f - g_A'^f\gamma^5)fZ'_\mu], \tag{21}$$

where f stands for a generic fermion. Using the results of Sec. II A and II B, we get

$$g_V^f = \cos\alpha_z\mathcal{G}_V^f + \sin\alpha_z\mathcal{H}_V^f,$$
$$g_V'^f = -\sin\alpha_z\mathcal{G}_V^f + \cos\alpha_z\mathcal{H}_V^f, \tag{22a}$$

$$g_A^f = \cos\alpha_z\mathcal{G}_A^f + \sin\alpha_z\mathcal{H}_A^f,$$
$$g_A'^f = -\sin\alpha_z\mathcal{G}_A^f + \cos\alpha_z\mathcal{H}_A^f, \tag{22b}$$

TABLE II. κ_x for different $U(1)_X$ models. Note that for the $B - L$ model our $U(1)_{B-L}$ charge differs from the conventional choice by a factor of $1/4$ due to our convention for the gauge coupling of the additional $U(1)_X$.

Model	$U(1)_{B-L}$	$U(1)_R$	$U(1)_\chi$	$U(1)_R \times U(1)_{B-L}$
Charge definitions	$\frac{(B-L)}{4}$	$-\frac{T_{3R}}{2}$	$-Q_\chi/\sqrt{10}$	$\frac{1}{5}[(B-L) - \frac{1}{2}T_{3R}]$
κ_x	$\frac{1}{4}$	0	$\frac{3}{20}$	$\frac{1}{5}$

TABLE III.   Coefficients entering in the fermionic couplings of Z and Z'.

Fermion (f)	Q^f	T_{3L}^f	p^f	r^f	s^f
u	+2/3	1/2	5/6	1/6	0
d	−1/3	−1/2	−1/6	1/6	0
e	−1	−1/2	−3/2	−1/2	0
ν_L	0	1/2	−1/2	−1/4	−1/4
N_R	0	0	0	−1/4	1/4

where

$$\mathcal{G}_V^f = -p^f + 2Q^f\frac{M_W^2}{M_{11}^2},$$

$$\mathcal{H}_V^f = p^f\mathcal{F} + r^f\frac{M_W}{M_{11}}\tan\theta_x, \tag{23}$$

and

$$\mathcal{G}_A^f = T_{3L}^f, \qquad \mathcal{H}_A^f = -T_{3L}^f\mathcal{F} + s^f\frac{M_W}{M_{11}}\tan\theta_x. \tag{24}$$

The quantities Q^f (electric charge), T_{3L}^f (third component of weak isospin of f_L), p^f, r^f, and s^f for the different fermions are listed in Table III. In Eqs. (23) and (24), $\mathcal{F}$ is given by

$$\mathcal{F} \equiv \frac{(M_{Z'}^2 - M_Z^2)}{M_{11}^2}\sin\alpha_z\cos\alpha_z. \tag{25}$$

Through Eqs. (22) to (25), the fermion couplings are expressed in terms of measurable quantities, and the characteristic model-independent constants are given in Table III.

For the left-handed neutrinos, for later use, we define $\kappa_{Z,Z'}$ through

$$g_V^\nu = g_A^\nu = \frac{\kappa_Z}{2}, \qquad g_V'^\nu = g_A'^\nu = \frac{\kappa_{Z'}}{2}. \tag{26}$$

It is to be noted that the vector and axial-vector couplings of Z and Z' to the fermions depend on three quantities: $M_{Z'}$, α_z and θ_x. What is interesting is that κ_x, which is a parameter characterizing different models in an anomaly-free gauged $U(1)_X$ setup, cancels out for all the couplings. Curiously, the prefactor of κ_x for each field is exactly twice its hypercharge (see Table I). The other contributions to the $U(1)_X$ charges, which depend on x_N, survive. Our choice that the right-handed neutrino, N_R, receives Majorana masses through coupling with S allowed us to set $x_N = -1/4$. Since all the observables can be determined in terms of the three unknowns $M_{Z'}$, α_z and θ_x, our formalism is completely model independent, as all model

dependence can be soaked within the above three quantities as long as we stick to an anomaly-free setup.[2]

III. BOUNDS FROM DIRECT SEARCHES AT THE LHC

The LHC experiments CMS and ATLAS routinely search for exotic neutral vector resonances going to $\ell^+\ell^-(\ell \equiv e, \mu, \tau)$ final states (DY modes). The nondiscovery of any such new particle to date translates to exclusion limits on the mass and couplings of the Z'. In this section, we extract such bounds using the latest 36 fb^{-1} ATLAS data [52] and cast them in a model-independent manner.

To analyze the constraints arising from direct resonant Z' production at the LHC, decaying to a pair of charged leptons, we first define the chiral couplings g_L^f and g_R^f through

$$g_R^f = \frac{g}{2\cos\theta_w}(g_V'^f - g_A'^f),$$
$$g_L^f = \frac{g}{2\cos\theta_w}(g_V'^f + g_A'^f). \quad (27)$$

From Eq. (26), we note that the right-handed couplings of the light neutrinos to Z', g_R^ν are zero. In writing Eq. (27), we have implicitly assumed flavor diagonal couplings for Z' but kept open the possibility of flavor nonuniversality. With this, the cross section for resonant production of a Z' boson at the LHC and its subsequent decay into a pair of charged leptons can be conveniently expressed as (in the narrow-width approximation, for illustration)[34][3]

$$\sigma(pp \to Z'X \to \ell^+\ell^-X) = \frac{\pi}{6s}\sum_q C_q^\ell w_q(s, M_{Z'}^2), \quad (28)$$

where the sum is over all the partons. The coefficients

$$C_q^\ell = [(g_L^q)^2 + (g_R^q)^2]\text{BR}(Z' \to \ell^+\ell^-) \quad (29)$$

involve the fermionic couplings of Z' and hence depend on the details of the fermionic sector of the model under consideration. The functions w_q, on the other hand, contain

all the information about the parton distribution functions (PDFs) and QCD corrections, detailed expressions for which appear in the Appendix. Considering the fact that w_u and w_d are substantially larger than the w_q functions for the other quarks, we can approximate Eq. (28) as follows[4]:

$$\sigma(pp \to Z'X \to \ell^+\ell^-X)$$
$$\approx \frac{\pi}{6s}[C_u^\ell w_u(s, M_{Z'}^2) + C_d^\ell w_d(s, M_{Z'}^2)]. \quad (30)$$

Direct searches at the LHC put upper limits on the left-hand side of Eq. (28). The most recent ATLAS limits can be found in Refs. [52,53], in which, as expected, the bound for the $\ell^\pm \equiv \tau^\pm$ case is less stringent than for $\ell^\pm \equiv e^\pm, \mu^\pm$. Using the CT14NLO PDF set [63], we evaluate w_u and w_d and translate the limit on the cross section into a bound in the C_u^ℓ-C_d^ℓ plane for different values of $M_{Z'}$. The results have been displayed in Fig. 1, in which the left panel corresponds to $\ell \equiv e, \mu$[5] and the right panel corresponds to $\ell \equiv \tau$. For any chosen $M_{Z'}$, only the interior of the corresponding contour is allowed. Although the bound arising from the $\tau^+\tau^-$ final state is substantially weaker compared to that from the e^+e^-, $\mu^+\mu^-$ final state, it may have its own advantage for scenarios in which, e.g., the Z' dominantly couples to the third generation of fermions [65–67].

IV. THEORETICAL CONSTRAINT FROM UNITARITY

For $U(1)$ extended models, in the absence of a Z', the scattering amplitude for the process $W_L^+W_L^- \to W_L^+W_L^-$, in which $W_L^\pm$ denotes the longitudinal component of the W boson, will grow as the fourth power of the center-of-momentum (CoM) energy at the leading order. To put it explicitly, if the Z' is too heavy to contribute, then we can write the Feynman amplitude for $W_L^+W_L^- \to W_L^+W_L^-$ as

$$\mathcal{M}_{W_L^+W_L^- \to W_L^+W_L^-} = \frac{g^2\cos^2\theta_w E^4}{M_W^4}\sin^2\alpha_z(-3 + 6\cos\theta + \cos^2\theta) + \mathcal{O}\left(\frac{E^2}{M_W^2}\right), \quad (31)$$

where E denotes the CoM energy and θ is the scattering angle. From Eq. (31), the $l = 0$ partial wave amplitude that usually gives the strongest bound can be extracted as

---

[2]We mention here the leptophobic Z' scenarios (mainly, E_6 models) advocated in Refs. [57–59]. Indeed, the leptonic couplings of X' can be made to vanish by appropriately tuning the kinetic mixing parameter χ. However, the relatively heavier mass eigenstate Z' ceases to be truly leptophobic as it invariably contains a part of the SM-like weak eigenstate through the unavoidably nonvanishing mixing angle α_Z in an anomaly-free setup. If instead we force the heavier state Z' to be purely leptophobic, we cannot avoid an untenable corollary that $\tan\theta_x = 0$, i.e., the extra $U(1)_X$ gauge coupling g_x has to vanish.

[3]The reader may notice a difference of a $1/8$ factor between our expression and the one given in Ref. [34]. This issue has been addressed in Refs. [60,61], the conventions of which we follow here.

[4]For most Z' models, this is a reasonable approximation. In particular, in models with flavor universal Z' couplings, we have checked that it hardly makes a visible difference if we use Eq. (28) instead of the approximate formula of Eq. (30). But, of course, this approximation breaks down in the extreme case when the Z' does not couple at all to the first generation of quarks [62].

[5]Such an analysis was carried out by CMS using their 8 TeV (20 fb^{-1}) dilepton data [64]. A comparison with our results shows that there is almost an order of magnitude improvement in the corresponding bounds, if we use the current 13 TeV (36 fb^{-1}) data.
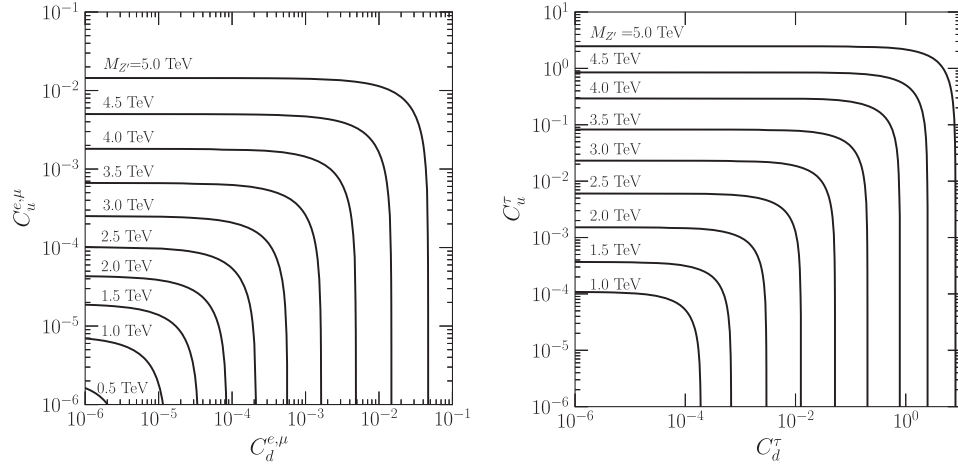
FIG. 1.   Exclusion contours at 95% C.L. in the C_u^ℓ-C_d^ℓ plane for different values of $M_{Z'}$, derived using ATLAS data for dilepton final states [52,53]. In the left panel, the contours are for the $\ell \equiv e, \mu$ final state, and the right panel corresponds to the $\tau^+\tau^-$ final state. For any given $M_{Z'}$, the interior of the corresponding contour is allowed.

$$a_0 = -\frac{8}{3}\frac{g^2 \cos^2\theta_w E^4}{M_W^4}\sin^2\alpha_z. \tag{32}$$

Unitarity restricts the magnitude of a_0 as $|a_0| < 8\pi$, which translates into an upper bound for the CoM energy,

$$E < E_{\max} = \left[8\pi \times \frac{3(M_Z^2\cos^2\alpha_z + M_{Z'}^2\sin^2\alpha_z)}{32\sqrt{2}G_F\sin^2\alpha_z}\right]^{\frac{1}{4}}, \tag{33}$$

where G_F is the Fermi constant obtained via the relation

$$g^2/M_W^2 = 4\sqrt{2}G_F, \tag{34}$$

and we have used Eq. (17a) to substitute for $M_W^2/\cos^2\theta_w$. Thus, to restore unitarity, effects of the Z' must set in before the CoM energy reaches $E_{\max}$, i.e., $M_{Z'} < E_{\max}$, which implies

$$\frac{M_{Z'}^4 \sin^2\alpha_z}{(M_Z^2\cos^2\alpha_z + M_{Z'}^2\sin^2\alpha_z)} < 8\pi \times \frac{3}{32\sqrt{2}G_F}. \tag{35}$$

To find a physical interpretation for the above bound, we write down the expression for the $Z' \rightarrow W^+W^-$ decay width as

$$\Gamma(Z' \rightarrow W^+W^-) \approx \frac{1}{64\pi}\frac{g^2\cos^2\theta_w\sin^2\alpha_z}{3}M_{Z'}\left(\frac{M_{Z'}}{M_W}\right)^4, \tag{36}$$

which is valid in the limit $M_{Z'} \gg M_W$ when the longitudinal components of the W bosons dominate [68,69]. Substituting for $\cos\theta_w$ using Eq. (17a), one can easily verify that this partial decay width increases with $\sin\alpha_z$ as well as $M_{Z'}$. However, the resonance should be narrow

enough so that it can be distinguished experimentally from the flat background. In view of this, it may be reasonable to impose a rather conservative limit,

$$\Gamma(Z' \rightarrow W^+W^-) < M_{Z'}. \tag{37}$$

Using Eqs. (17a) and (34), one can check that the above bound can be translated into

$$\frac{M_{Z'}^4 \sin^2\alpha_z}{(M_Z^2 \cos^2\alpha_z + M_{Z'}^2 \sin^2\alpha_z)} < 48\pi \times \frac{1}{\sqrt{2}G_F}, \tag{38}$$

which is slightly weaker than the unitarity bound in Eq. (35). Therefore, consideration of unitarity implicitly keeps the corresponding partial decay width under control.[6]

The tree unitarity constraint is of prime importance as it translates to an *upper bound* on $M_{Z'}$, for a given $\sin\alpha_z$, complementing the lower bound that comes from direct search experiments. This can be seen from Eq. (35).[7] We show this explicitly when we discuss the interplay of the different bounds in Sec. VI. It should also be noted that, although unitarity in the context of Z' models has been studied earlier [73,74], to our knowledge, the possibility of using it to cast an upper bound on the Z' mass as in Eq. (35) has not been emphasized before and thus constitutes a new

---

[6]It is worth remarking that such a lesser-known virtue of the unitarity bound is also present in the case of the SM Higgs boson. For $m_h \gg M_W$, $\Gamma(h^{SM} \rightarrow W^+W^-)$ grows as m_h^3 and would equal m_h for $m_h \approx 1.4$ TeV [70]. But the bound $m_h < 1$ TeV from the $W_L^+W_L^-$ scattering ensures that such a situation never arises.

[7]Similarly for $f\bar{f} \rightarrow W_L^+W_L^-$, the scattering amplitude will grow as $\mathcal{O}(E^2)$ [71] and can give an upper bound on $M_{Z'}$ for nonzero α_z. But this bound will depend on the fermionic couplings of Z' [72] and will not be as model independent.

observation in our paper. Moreover, since this analysis does not depend on the details of the fermionic couplings, such a bound is quite general and can be applied to a wide class of Z' models.

V. CONSTRAINTS FROM ν_μ-e SCATTERING

The unitarity constraint, described in the previous section, relies on sniffing the effects of Z' through the Z-Z' mixing. Therefore, the bounds are lifted in the limit $\sin\alpha_z = 0$ as has been clearly depicted in Fig. 2. However, depending on how Z' couples to the fermions, it is possible to put lower bounds on $M_{Z'}$, even in the limit of vanishing Z-Z' mixing [75,76]. This can be done, e.g., by using the data from low-energy neutrino-electron scattering such as $\nu_\mu e \to \nu_\mu e$, which proceeds at the tree level purely via neutral current (see, e.g., Refs. [74,77,78]). In models with an extra $U(1)$, the Z' boson will, in general, also contribute to the scattering.

The dimension-6 operator governing $\nu_\mu - e$ scattering at low energies is written as

$$\mathcal{L}_{\nu e} = -\frac{G_F}{\sqrt{2}}[\bar{\nu}\gamma^\mu(1-\gamma^5)\nu][\bar{e}\gamma_\mu(g_V^{\nu e} - g_A^{\nu e}\gamma^5)e]. \quad (39)$$

We recall that in the SM the expressions for $g_V^{\nu e}$ and $g_A^{\nu e}$ are very simple at the tree level and are given by

$$(g_V^{\nu e})^{\text{SM}} \equiv (g_V^e)^{\text{SM}} = -\frac{1}{2} + 2\sin^2\theta_w,$$

$$(g_A^{\nu e})^{\text{SM}} \equiv (g_A^e)^{\text{SM}} = -\frac{1}{2}. \quad (40)$$

Of course, in the Z' models under consideration, the above expressions will be modified [see Eq. (26)] as

$$(g_{(V,A)}^{\nu e})^{\text{model}} = M_{11}^2\left(\frac{\kappa_Z g_{(V,A)}^e}{M_Z^2} + \frac{\kappa_{Z'} g_{(V,A)}^{\prime e}}{M_{Z'}^2}\right), \quad (41)$$

where the expression for M_{11}^2 appears in Eq. (17) and the rest of the couplings appear in Eq. (22).

We use this formula along with the global fit values from PDG [79]

$$g_V^{\nu e} = -0.040 \pm 0.015, \qquad g_A^{\nu e} = -0.507 \pm 0.014 \quad (42)$$

to draw the 2σ allowed regions in the $\sin\alpha_z$-$M_{Z'}$ plane for two different values of $\tan\theta_x$ as shown by the blue curves in Fig. 2.

VI. RESULTS AND DISCUSSIONS

Until now, we have developed a general formalism on how to constrain a minimal Z' model from theoretical considerations as well as from different types of experimental data. Now, we combine the different limits together, described in the previous sections, to obtain stronger bounds on the parameter space. To illustrate,
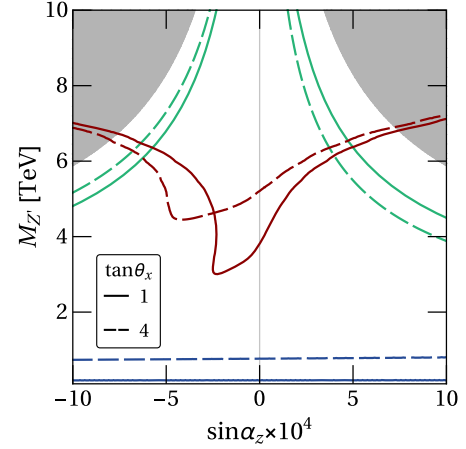
FIG. 2. Consolidated bounds in the $(\sin\alpha_z$-$M_{Z'})$ plane for anomaly-free $U(1)_X$ models. The shaded region is excluded from unitarity. The red and the blue colors indicate the limits set by direct detection and ν_μ-e scattering data, respectively. The green contours are obtained by setting $\Gamma_{Z'} = M_{Z'}/2$. The solid and dashed line types correspond to $\tan\theta_x = 1$ and 4, respectively. The region above the red lines is allowed by the 36 fb^{-1} ATLAS data, whereas the region above the blue lines and the interior of the green contours represent the allowed area from the ν_μ-e scattering data and $\Gamma_{Z'} \leq M_{Z'}/2$, respectively.

$C_{u,d}^{e,\mu}$ and $g_V^{\nu e}$[8] can be determined, using Eqs. (29), (27), and (41) in conjunction with Eq. (22), in terms of the three quantities $M_{Z'}$, α_z, and $\tan\theta_x$. The bound from the left panel of Fig. 1 and the constraint coming from ν_μ-e scattering can then be translated to the limits on those three parameters.

In Fig. 2, these bounds have been displayed in the $\sin\alpha_z$-$M_{Z'}$ plane for any anomaly-free $U(1)_X$ model for two typical choices of $\tan\theta_x$. The region excluded from unitarity has been shaded in gray and is independent of $\tan\theta_x$. The lower bounds on $M_{Z'}$, arising from the ATLAS (13 TeV, 36 fb^{-1}) exclusion of the DY production of Z', are depicted as red curves, whereas the region above the light blue curves denotes the region consistent with ν_μ-e scattering. Additionally, we also give contours that represent a constraint on the Z' decay width, as a guideline for the validity of a particle interpretation. The green lines in the figure arise from the consideration[9] $\Gamma_{Z'} \leq M_{Z'}/2$.

For all the colored contours, the solid (dashed) curves correspond to $\tan\theta_x = 1(4)$. Recall that $\tan\theta_x$ is proportional to the effective $U(1)_X$ coupling, g'_x. As it happens, the lower bounds on $M_{Z'}$ arising from low-energy ν_μ-e

---

[8]Using the expressions in Eq. (22), we have checked that $g_A^{\nu e} = -0.5$ is independent of the model parameters.
[9]What constitutes an acceptable width of a heavy particle, or how far the narrow-width approximation holds well, can be a matter of discussion, and hence we choose to veer on the conservative side, to illustrate what role the consideration of width might play in restricting the parameter space.

TABLE IV. Summary of bounds on $M_{Z'}$ and α_z for anomaly-free $U(1)_X$ models using two representative values of $\tan\theta_x$ [which is proportional to the effective $U(1)_X$ coupling].

	Maximum $|\sin\alpha_z|$	10^{-3}
$\tan\theta_x = 4$	$M_{Z'}$ exclusion at $\alpha_z = 0$ (TeV)	5.1
	Lowest possible value of $M_{Z'}$ (TeV)	4.4
	Maximum $|\sin\alpha_z|$	10^{-3}
$\tan\theta_x = 1$	$M_{Z'}$ exclusion at $\alpha_z = 0$ (TeV)	3.8
	Lowest possible value of $M_{Z'}$ (TeV)	3.0

scattering are considerably weaker than those from direct searches. However, ν_μ-e scattering can put important constraints on hadrophobic Z' models when the production of the Z' at the LHC is very suppressed. Combining the lower bound on $M_{Z'}$ from the direct searches with the corresponding upper bound coming from, e.g., unitarity, we are able to extract an upper limit on the magnitude of the Z-Z' mixing angle, α_z. Such bounds on $|\alpha_z|$ are on par with the corresponding limits from electroweak precision data [47,80].

In Table IV, we have summarized the bounds on α_z and $M_{Z'}$ for $\tan\theta_x = 1$ and 4 for anomaly-free $U(1)_X$ models. From Table II, we recall that the choice $\tan\theta_x = 4$ corresponds to $g'_x = g$ for the "conventional" $(B - L)$ model. This is so because for $(B - L)$ model in our normalization $\kappa_x = 1/4$, and $g'_x \kappa_x$ in our setup is equivalent to a generic g'_x in the conventional $(B - L)$ model. It should be pointed out that, although we have taken into account the decays $Z' \to W^+W^-$ and $Z' \to Zh$ (h being the lighter SM-like Higgs scalar) for our analysis, we have assumed the decays $Z' \to NN$, where N denotes a heavy RH neutrino, and $Z' \to ZH$, where H is the heavier nonstandard scalar, to be kinematically forbidden. The lower bound on $M_{Z'}$ is likely to be diluted further if these decay channels open up.

It may be useful to note that every point in the $\sin\alpha_z$-$M_{Z'}$ plane in Fig. 2 corresponds, through Eq. (25), to a definite value of $\mathcal{F}$. If a specific model is chosen, then one can use the relation

$$\tan\chi = \left(2\kappa_x - \frac{1}{2}\right)\tan\theta_x \cot\theta_w - \frac{\mathcal{F}}{\sin\theta_w}, \quad (43)$$

which follows from Eq. (17c), to determine the kinetic mixing angle, χ, corresponding to this point. The value of κ_x varies from model to model, $\tan\theta_x$ is a measure of the effective gauge coupling of the extra $U(1)_X$, and $\cos\theta_w$ is determined in terms of $\sin\alpha_z$ and $M_{Z'}$ through Eq. (17). Conversely, for a fixed value of the kinetic mixing parameter, χ, any model would correspond to a curve, determined by κ_x, in the $\sin\alpha_z$-$M_{Z'}$ plane. For a definite example, if we consider the $(B - L)$ model ($\kappa_x = 1/4$), the curve corresponding to $\chi = 0$ is a vertical straight line through the origin. This is reminiscent of the fact that in this model Z-Z' mixing is entirely due to kinetic mixing.
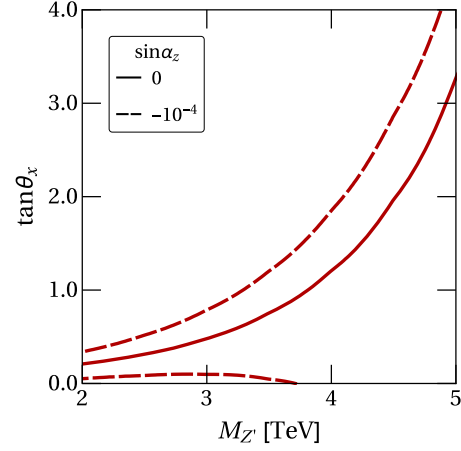
FIG. 3. Bounds in the $(M_{Z'}$-$\tan\theta_x)$ plane for anomaly-free $U(1)_X$ models using two representative values of $\sin\alpha_z$, namely, 0 and (-10^{-4}). For these choices of $\sin\alpha_z$ the strongest limits arise from the direct searches, which have been displayed as the red lines. For $\sin\alpha_z = 0$, the region to the right of the solid red curve is allowed, whereas for $\sin\alpha_z = (-10^{-4})$, the allowed region lies within the dashed red curves.

In Fig. 3, we take a complementary approach by casting the bounds in the $M_{Z'}$-$\tan\theta_x$ plane, for two representative values of $\sin\alpha_z$, namely, 0 and (-10^{-4}). For these values of $\sin\alpha_z$, the strongest limits come from direct searches, which have been displayed by the red lines. For $\sin\alpha_z = 0$, the region to the right of the solid red line is allowed, whereas for $\sin\alpha_z = (-10^{-4})$, the region contained within the dashed red lines is allowed. The absence of contours from considerations of unitarity and $\nu_\mu - e$ scattering in Fig. 3 implies that the corresponding curves are too weak to enter inside the zoomed range of the parameter space.

In Fig. 4, we display the bounds in the $\sin\alpha_z$-$\tan\theta_x$ plane, for two representative values of $M_{Z'}$, namely, 4 and 5 TeV. For these values of $M_{Z'}$, the strongest limits come from direct searches, displayed by the red lines. For $M_{Z'} = 4$ TeV, the region inside the solid red contour is allowed, whereas for $M_{Z'} = 5$ TeV, the region bounded within the dashed red lines is allowed. The green lines correspond to $\Gamma_{Z'} \leq M_{Z'}/2$.

Finally, with the ambitious expectation that a Z' will be discovered in future, in Fig. 5, we illustrate how model-specific information can be extracted using the following hypothetical measurements of the model-independent parameters:

$$M_{Z'} \approx 5.5 \text{ TeV}, \quad \sin\alpha_z \approx (-10^{-4}), \quad \tan\theta_x \approx 1. \quad (44)$$

The solid black line in Fig. 5 has been obtained by combining Eqs. (9b) and (9c) for $\tan\theta_x = 1$. It does not depend on the chosen model. The red lines, on the other hand, are drawn using Eq. (9d) in conjunction with Eqs. (17a) and (17c) to trade
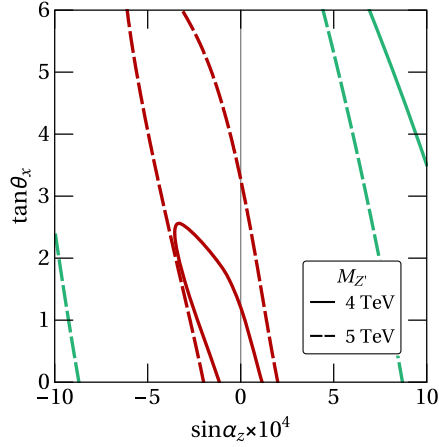
FIG. 4. Consolidated bounds in the $(\sin \alpha_z - \tan \theta_x)$ plane for anomaly-free $U(1)_X$ models using two representative values of $M_{Z'}$, namely, 4 and 5 TeV. For these values of $M_{Z'}$, the strongest limits come from direct searches, displayed by the red lines. For $M_{Z'} = 4$ TeV, the region inside the solid red contour is allowed, whereas for $M_{Z'} = 5$ TeV, the region bounded within the dashed red lines is allowed. The green lines refer to $\Gamma_{Z'} \leq M_{Z'}/2$ for which the limits are rather weak for the chosen values of $M_{Z'}$ (the region inside the dashed lines is allowed for $M_{Z'} = 5$ TeV, while for $M_{Z'} = 4$ TeV, only one side of the contour, the solid line, is visible).

θ_w and x'_Φ in favor of $M_{Z'}$, α_z, and $\tan \theta_x$. Since the red lines require the input of x_Φ, which, in turn, depends on κ_x, the lines are different for different models. The intersection of the black line with a particular red line gives the solutions for the kinetic mixing parameter, χ, and the $U(1)_X$ coupling, g_x, for that particular model. Such a solution might provide intuition as to whether a specific $U(1)_X$ model fits into a more
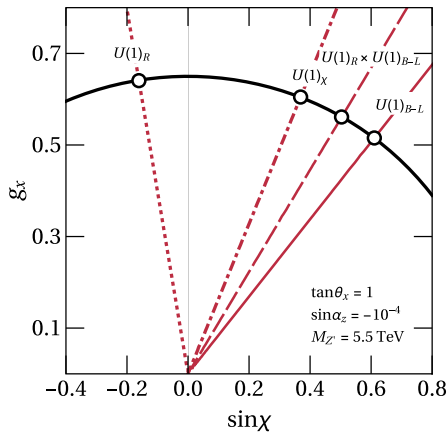
FIG. 5. Example plot illustrating the inter-relationship between kinetic mixing $(\sin \chi)$ and the original $U(1)_X$ coupling (g_x) assuming hypothetical measurements: $M_{Z'} \approx 5.5$ TeV, $\sin \alpha_z \approx (-10^{-4})$, and $\tan \theta_x \approx 1$. The solid black curve is the contour corresponding to Eq. (9c). Each red line corresponds to a particular model, drawn in conformity with Eqs. (9d) and (17c). The intersection of the black curve with a particular red line gives the solutions for the kinetic mixing and g_x for a given model.

elaborate scheme, such as grand unification, at higher energies.

VII. CONCLUSIONS

Our intention in this paper has been to put constraints on the parameter space of the minimal extension of the SM with an additional gauged $U(1)$ giving a massive neutral Z' gauge boson. We did revisit the formalism first to set up the notations. We have advocated a parametrization in which, in the presence of kinetic mixing, the constraints on different anomaly-free $U(1)_X$ models can be expressed in a model-independent unified framework. Importantly, we have not *a priori* assumed, unlike most of the previous works, that the Z-Z' mixing angle is small or the Z' mass is way above the Z mass. For the sake of illustration, we explicitly examine a few popular scenarios of $U(1)$ extension, e.g., the $(B - L)$ model, an $U(1)$ arising from left-right symmetry, etc. It turns out that there are three important quantities to be determined that cover the extended parameter space and absorb all model dependence for a nonanomalous $U(1)$ extension. These quantities are the mass of the Z', the effective gauge coupling strength (g'_x) of the extra $U(1)$, and the Z-Z' mixing angle (α_z). To constrain this space, we have primarily employed three types of information, namely, the LHC (ATLAS) 13 TeV Drell-Yan data with 36 fb^{-1} luminosity, the results from low-energy $\nu_\mu - e$ scattering, and consistency with s-wave unitarity in the $W_L^+ W_L^- \to W_L^+ W_L^-$ channel. The LHC data turn out to be most constraining. We also observe that constraints on the Z' decay width, $\Gamma_{Z'}$, translate to constraints in the parameter space which are *similar in nature* to those obtained from s-wave unitarity. We want to underscore that, although we employ the anomaly-free (per generation) models to exemplify our formalism, the analysis can in general be used to constrain other extensions of the SM with an additional Z'. The interplay between the different bounds can be used to constrain models with or without couplings to fermions, and with or without Z-Z' mixing. Also, models with a Z' that couples only to leptons, or even preferentially to the third generation, can be constrained using our study. The new things that emerge from our analysis are the following:

(i) Our parametrization shows that increasingly precise experimental data would squeeze the allowed region in the three-dimensional space of $M_{Z'}$, α_z, and θ_x. The description is completely model independent as long as the fermion content ensures an anomaly-free setup. Model dependence is encoded in κ_x, which is different for different models, as listed in Table II. Of the other parameters, the strength of kinetic mixing, χ, should in principle be a derived quantity in a fundamental theory given the charges of a possible set of heavy particles (couplings both to B_μ and X_μ), integrated out to generate the mixing. Nevertheless, in our approach, which is agnostic toward models of UV completion, χ is treated as an effective parameter. Given a model (i.e., a value of κ_x), one can

calculate a range in χ using Eq. (43), which would fit values (or limits) of $M_{Z'}$, α_z, and θ_x extracted directly from experimental data.

(ii) We have updated the model-independent constraints in the C_u^ℓ-C_d^ℓ ($\ell \equiv e, \mu$) plane, using the latest 13 TeV (36 fb^{-1}) ATLAS data. We obtain an improvement of 1 order of magnitude over the previous constraints in the same plane obtained from the publicly available 7–8 TeV CMS results [64] (see also Ref. [37]) and several orders of magnitude over those from Tevatron results [34]. While constraints were speculated before actual LHC data arrived [10,35,36], our analysis provides the most updated ones in the C_u^ℓ-C_d^ℓ plane using the latest publicly available LHC (ATLAS) data. Translating experimental data to constraints in the above plane as a function of $(M_{Z'}, C_u^\ell, C_d^\ell)$, rather than directly to limits on $M_{Z'}/g_x'^2$, is quite useful as it provides a model-independent platform from where limits on any type of specific customized models can be easily extracted. ATLAS has also provided bounds for Drell-Yan $\tau^+\tau^-$ production through a Z'. We use this data set to set similar constraints in the C_u^τ-C_d^τ plane. Though less restrictive, these latter bounds are useful for nonuniversal Z' models that have a different coupling to the third-generation fermions.

(iii) The s-wave unitarity constraints in the ($M_{Z'}$-$\sin \alpha_z$) plane, placed for the first time in this paper, turn out to provide complementary limits when the LHC direct search and the low-energy ν_μ-e scattering constraints are superposed in the same plane. It is important to observe that the unitarity constraints are insensitive to the extra $U(1)$ coupling strength, g_x', and in conjunction with the LHC direct search limits, they restrict the Z-Z' mixing to be small (which we have not _a priori_ assumed). However, when we require $\Gamma_{Z'} \leq 0.5 M_{Z'}$, the constraints turn out to be much stronger than the ones obtained from ν_μ-e scattering data or from satisfying s-wave unitarity. The constraints on the mixing angle (α_z) we obtain are, in fact, of the same order as obtained from electroweak precision tests [47,80].

(iv) When the Z' couples to fermions with the same strength as that of the SM $SU(2)_L$ gauge boson [for the $(B-L)$ model, this corresponds to $\tan \theta_x = 4$), we obtain $M_{Z'} > 4.4$ TeV and $|\alpha_z| < 0.001$ at 95% C.L.

We urge our experimental colleagues to take notice of our assertion that a model-independent analysis, as depicted especially by the direct detection contour in Fig. 2, can be carried out with just three independent parameters, as discussed in detail.

ACKNOWLEDGMENTS

Note added—Recently, the 13 TeV Drell-Yan data from the CMS Collaboration became available [81]. Our result in the $C_u^{e,\mu}$-$C_d^{e,\mu}$ plane, which uses the 13 TeV ATLAS Drell-Yan data, is very similar to that obtained by the CMS Collaboration. Analysis using the 13 TeV ATLAS Drell-Yan data has also been performed very recently in Refs. [82,83].

APPENDIX: DETAILED EXPRESSIONS FOR w_q

The next-to-leading-order expressions for the functions, w_q, which appear in Eq. (28), are given by

$$w_q(s, M_{Z'}^2) = \int_0^1 dx \int_0^1 dy \int_0^1 dz \delta\left(\frac{M_{Z'}^2}{s} - xyz\right)$$
$$\times \{F_{qq}(x, y, M_{Z'}^2)\Delta_{qq}(z, M_{Z'}^2)$$
$$+ F_{gq}(x, y, M_{Z'}^2)\Delta_{gq}(z, M_{Z'}^2)\}, \quad (A1)$$

For pp colliders such as the LHC, we have[34]

$$F_{qq}(x,y,M_{Z'}^2) = f_{q\leftarrow P}(x,M_{Z'}^2)f_{\bar{q}\leftarrow P}(y,M_{Z'}^2) + (x \leftrightarrow y), \quad (A2a)$$

$$F_{gq}(x,y,M_{Z'}^2) = f_{g\leftarrow P}(x,M_{Z'}^2)[f_{q\leftarrow P}(y,M_{Z'}^2)$$
$$+ f_{\bar{q}\leftarrow P}(y,M_{Z'}^2)] + (x \leftrightarrow y), \quad (A2b)$$

where $f_{q\leftarrow P}(x, M_{Z'}^2)$ represents the PDF for the parton q at a factorization scale, $M_{Z'}$. The scaling functions, Δ_{qq} and Δ_{gq}, are given by [84]

$$\Delta_{qq}(z, M_{Z'}^2) = \delta(1 - z) + \frac{\alpha_s(M_{Z'}^2)}{\pi} C_F\left[\left(\frac{\pi^2}{3} - 4\right)\delta(1 - z)\right.$$
$$- \frac{1+z^2}{1-z}\ln(z) - 2(1+z)\ln(1-z)$$
$$\left. + 4(1+z^2)\left(\frac{\ln(1-z)}{1-z}\right)_+\right], \quad (A3a)$$

$$\Delta_{gq}(z, M_{Z'}^2) = \frac{\alpha_s(M_{Z'}^2)}{2\pi} T_F\left[(1 - 2z + 2z^2)\ln\frac{(1-z)^2}{z} + \frac{1}{2}\right.$$
$$\left. + 3z - \frac{7}{2}z^2\right], \quad (A3b)$$

where $C_F = 4/3$ and $T_F = 1/2$ are the quark and gluon color factors, respectively. The plus prescription is defined as follows:

$$\int_0^1 dx f(x)g(x)_+ = \int_0^1 dx[f(x) - f(1)]g(x). \quad (A4)$$

We obtained our numerical results using these equations.

[1] J. C. Pati and A. Salam, Is Baryon Number Conserved?, Phys. Rev. Lett. **31**, 661 (1973).

[2] J. C. Pati and A. Salam, Lepton number as the fourth color, Phys. Rev. D **10**, 275 (1974); Erratum **11**, 703(E) (1975).

[3] R. N. Mohapatra and J. C. Pati, Natural left-right symmetry, Phys. Rev. D **11**, 2558 (1975).

[4] G. Senjanovic and R. N. Mohapatra, Exact left-right symmetry and spontaneous violation of parity, Phys. Rev. D **12**, 1502 (1975).

[5] H. Georgi, The state of the art gauge theories, AIP Conf. Proc. **23**, 575 (1975).

[6] H. Fritzsch and P. Minkowski, Unified interactions of leptons and hadrons, Ann. Phys. (N.Y.) **93**, 193 (1975).

[7] F. Gursey, P. Ramond, and P. Sikivie, A universal gauge theory model based on E6, Phys. Lett. **60B**, 177 (1976).

[8] D. London and J. L. Rosner, Extra gauge bosons in E(6), Phys. Rev. D **34**, 1530 (1986).

[9] P. Langacker, Grand unified theories and proton decay, Phys. Rep. **72**, 185 (1981).

[10] T. G. Rizzo, Z' phenomenology and the LHC, in *Proceedings of Theoretical Advanced Study Institute in Elementary Particle Physics: Exploring New Frontiers Using Colliders and Neutrinos (TASI 2006)* (World Scientific, Singapore, 2008), p. 537.

[11] J. L. Hewett and T. G. Rizzo, Low-energy phenomenology of superstring inspired E(6) models, Phys. Rep. **183**, 193 (1989).

[12] M. Cvetic and P. Langacker, Implications of Abelian extended gauge structures from string models, Phys. Rev. D **54**, 3570 (1996).

[13] A. Leike, The phenomenology of extra neutral gauge bosons, Phys. Rep. **317**, 143 (1999).

[14] P. Langacker, The physics of heavy Z' gauge bosons, Rev. Mod. Phys. **81**, 1199 (2009).

[15] N. Arkani-Hamed, A. G. Cohen, and H. Georgi, Electroweak symmetry breaking from dimensional deconstruction, Phys. Lett. B **513**, 232 (2001).

[16] M. Perelstein, Little Higgs models and their phenomenology, Prog. Part. Nucl. Phys. **58**, 247 (2007).

[17] Y. Shadmi and Y. Shirman, Dynamical supersymmetry breaking, Rev. Mod. Phys. **72**, 25 (2000).

[18] I. Antoniadis, A possible new dimension at a few TeV, Phys. Lett. B **246**, 377 (1990).

[19] T. Appelquist, H.-C. Cheng, and B. A. Dobrescu, Bounds on universal extra dimensions, Phys. Rev. D **64**, 035002 (2001).

[20] K. Agashe, A. Delgado, M. J. May, and R. Sundrum, RS1, custodial isospin and precision tests, J. High Energy Phys. 08 (2003) 050.

[21] S. Iso, N. Okada, and Y. Orikasa, The minimal B-L model naturally realized at TeV scale, Phys. Rev. D **80**, 115007 (2009).

[22] S. Oda, N. Okada, D. Raut, and D.-s. Takahashi, Non-minimal quartic inflation in classically conformal $U(1)_X$ extended standard model, Phys. Rev. D **97**, 055001 (2018).

[23] A. Achucarro and T. Vachaspati, Semilocal and electroweak strings, Phys. Rep. **327**, 347 (2000).

[24] E. Dudas, Y. Mambrini, S. Pokorski, and A. Romagnoni, (In)visible Z-prime and dark matter, J. High Energy Phys. 08 (2009) 014.

[25] E. Dudas, Y. Mambrini, S. Pokorski, and A. Romagnoni, Extra U(1) as natural source of a monochromatic gamma ray line, J. High Energy Phys. 10 (2012) 123.

[26] R. Foot and S. Vagnozzi, Dissipative hidden sector dark matter, Phys. Rev. D **91**, 023512 (2015).

[27] R. Foot and S. Vagnozzi, Diurnal modulation signal from dissipative hidden sector dark matter, Phys. Lett. B **748**, 61 (2015).

[28] N. Okada and S. Okada, Z'-portal right-handed neutrino dark matter in the minimal $U(1)_X$ extended standard model, Phys. Rev. D **95**, 035025 (2017).

[29] N. Okada, S. Okada, and D. Raut, $SU(5) \times U(1)_X$ grand unification with minimal seesaw and Z'-portal dark matter, Phys. Lett. B **780**, 422 (2018).

[30] S. Okada, Z' portal dark matter in the minimal $B - L$ model, Adv. Ser. Dir. High Energy Phys., **2018**, 5340935 (2018).

[31] B. Kors and P. Nath, A Stueckelberg extension of the standard model, Phys. Lett. B **586**, 366 (2004).

[32] A. Berlin, D. Hooper, and S. D. McDermott, Simplified dark matter models for the Galactic Center gamma-ray excess, Phys. Rev. D **89**, 115022 (2014).

[33] J. M. Cline, G. Dupuis, Z. Liu, and W. Xue, The windows for kinetically mixed Z'-mediated dark matter and the galactic center gamma ray excess, J. High Energy Phys. 08 (2014) 131.

[34] M. Carena, A. Daleo, B. A. Dobrescu, and T. M. P. Tait, Z' gauge bosons at the Tevatron, Phys. Rev. D **70**, 093009 (2004).

[35] F. Petriello and S. Quackenbush, Measuring Z' couplings at the CERN LHC, Phys. Rev. D **77**, 115004 (2008).

[36] E. Salvioni, G. Villadoro, and F. Zwirner, Minimal Z-prime models: Present bounds and early LHC reach, J. High Energy Phys. 11 (2009) 068.

[37] E. Accomando, A. Belyaev, L. Fedeli, S. F. King, and C. Shepherd-Themistocleous, Z' physics with early LHC data, Phys. Rev. D **83**, 075012 (2011).

[38] M. R. Buckley, D. Hooper, J. Kopp, and E. Neil, Light Z' bosons at the Tevatron, Phys. Rev. D **83**, 115013 (2011).

[39] E. Accomando, C. Coriano, L. Delle Rose, J. Fiaschi, C. Marzo, and S. Moretti, Z', Higgses and heavy neutrinos in $U(1)'$ models: From the LHC to the GUT scale, J. High Energy Phys. 07 (2016) 086.

[40] N. Okada and S. Okada, Z'_{BL} portal dark matter and LHC Run-2 results, Phys. Rev. D **93**, 075003 (2016).

[41] A. De Simone, G. F. Giudice, and A. Strumia, Benchmarks for dark matter searches at the LHC, J. High Energy Phys. 06 (2014) 081.

[42] O. Buchmueller, M. J. Dolan, S. A. Malik, and C. McCabe, Characterising dark matter searches at colliders and direct detection experiments: Vector mediators, J. High Energy Phys. 01 (2015) 037.

[43] O. Ducu, L. Heurtier, and J. Maurer, LHC signatures of a Z' mediator between dark matter and the SU(3) sector, J. High Energy Phys. 03 (2016) 006.

[44] M. Klasen, F. Lyonnet, and F. S. Queiroz, NLO + NLL collider bounds, Dirac fermion and scalar dark matter in the BL model, Eur. Phys. J. C **77**, 348 (2017).

[45] R. Gauld, F. Goertz, and U. Haisch, On minimal Z' explanations of the $B \to K^*\mu^+\mu^-$ anomaly, Phys. Rev. D **89,** 015005 (2014).

[46] A. J. Buras and J. Girrbach, Left-handed Z' and Z FCNC quark couplings facing new $b \to s\mu^+\mu^-$ data, J. High Energy Phys. 12 (2013) 009.

[47] J. Erler, P. Langacker, S. Munir, and E. Rojas, Improved constraints on Z-prime bosons from electroweak precision data, J. High Energy Phys. 08 (2009) 017.

[48] G. Bhattacharyya, A. Datta, S. N. Ganguli, and A. Raychaudhuri, Z—Z-prime mixing in extended gauge models from LEP 1990 data, Mod. Phys. Lett. A **06,** 2557 (1991).

[49] G. Bhattacharyya, A. Raychaudhuri, A. Datta, and S. N. Ganguli, Z Decay Confronts Nonstandard Scenarios, Phys. Rev. Lett. **64,** 2870 (1990).

[50] R. H. Benavides, L. Muoz, W. A. Ponce, O. Rodrguez, and E. Rojas, Electroweak couplings and LHC constraints on alternative Z' models in E_6, arXiv:1801.10595.

[51] A. Ekstedt, R. Enberg, G. Ingelman, J. Lfgren, and T. Mandal, Constraining minimal anomaly free U(1) extensions of the Standard Model, J. High Energy Phys. 11 (2016) 071.

[52] M. Aaboud *et al.* (ATLAS Collaboration), Search for new high-mass phenomena in the dilepton final state using 36 fb^{-1} of proton-proton collision data at $\sqrt{s} = 13$ TeV with the ATLAS detector, J. High Energy Phys. 10 (2017) 182.

[53] M. Aaboud *et al.* (ATLAS Collaboration), Search for additional heavy neutral Higgs and gauge bosons in the ditau final state produced in 36 fb^{-1} of pp collisions at $\sqrt{s} = 13$ TeV with the ATLAS detector, J. High Energy Phys. 01 (2018) 055.

[54] B. Holdom, Two U(1)'s and epsilon charge shifts, Phys. Lett. **166B,** 196 (1986).

[55] K. S. Babu, C. F. Kolda, and J. March-Russell, Implications of generalized Z—Z-prime mixing, Phys. Rev. D **57,** 6788 (1998).

[56] B. Brahmachari and A. Raychaudhuri, Perturbative generation of $theta_{13}$ from tribimaximal neutrino mixing, Phys. Rev. D **86,** 051302 (2012).

[57] K. S. Babu, C. F. Kolda, and J. March-Russell, Leptophobic U(1) s and the R(b)-R(c) crisis, Phys. Rev. D **54,** 4635 (1996).

[58] C.-W. Chiang, T. Nomura, and K. Yagyu, Phenomenology of E_6-inspired leptophobic Z' boson at the LHC, J. High Energy Phys. 05 (2014) 106.

[59] J. Y. Araz, G. Corcella, M. Frank, and B. Fuks, Loopholes in Z' searches at the LHC: Exploring supersymmetric and leptophobic scenarios, J. High Energy Phys. 02 (2018) 092.

[60] D. Feldman, Z. Liu, and P. Nath, The Stueckelberg Z prime at the LHC: Discovery potential, signature spaces and model discrimination, J. High Energy Phys. 11 (2006) 007.

[61] G. Paz and J. Roy, A comment on the Z' Drell-Yan cross section, Phys. Rev. D **97,** 075025 (2018).

[62] A. A. Andrianov, P. Osland, A. A. Pankov, N. V. Romanenko, and J. Sirkka, On the phenomenology of a Z' coupling only to third family fermions, Phys. Rev. D **58,** 075001 (1998).

[63] S. Dulat, T.-J. Hou, J. Gao, M. Guzzi, J. Huston, P. Nadolsky, J. Pumplin, C. Schmidt, D. Stump, and C. P. Yuan, New parton distribution functions from a global analysis of quantum chromodynamics, Phys. Rev. D **93,** 033006 (2016).

[64] V. Khachatryan *et al.* (CMS Collaboration), Search for physics beyond the standard model in dilepton mass spectra in proton-proton collisions at $\sqrt{s} = 8$ TeV, J. High Energy Phys. 04 (2015) 025.

[65] D. J. Muller and S. Nandi, Top flavor: A separate SU(2) for the third family, Phys. Lett. B **383,** 345 (1996).

[66] K. R. Lynch, E. H. Simmons, M. Narain, and S. Mrenna, Finding Z' bosons coupled preferentially to the third family at LEP and the Tevatron, Phys. Rev. D **63,** 035006 (2001).

[67] R. Benavides, L. A. Muoz, W. A. Ponce, O. Rodrguez, and E. Rojas, Minimal nonuniversal electroweak extensions of the standard model: A chiral multiparameter solution, Phys. Rev. D **95,** 115018 (2017).

[68] F. del Aguila, M. Quiros, and F. Zwirner, On the mass and the signature of a new Z, Nucl. Phys. **B284,** 530 (1987).

[69] N. G. Deshpande and J. Trampetic, Decay of Z' in W^+W^- and Higgs modes, Phys. Lett. B **206,** 665 (1988).

[70] J. F. Gunion, H. E. Haber, G. L. Kane, and S. Dawson, *The Higgs Hunter's Guide*, Frontiers of Physics series (Westview Press, 2000).

[71] G. Bhattacharyya, D. Das, and P. B. Pal, Modified Higgs couplings and unitarity violation, Phys. Rev. D **87,** 011702 (2013).

[72] K. S. Babu, J. Julio, and Y. Zhang, Perturbative unitarity constraints on general W' models and collider implications, Nucl. Phys. **B858,** 468 (2012).

[73] K. Cheung, C.-W. Chiang, Y.-K. Hsiao, and T.-C. Yuan, Longitudinal weak gauge bosons scattering in hidden Z-prime models, Phys. Rev. D **81,** 053001 (2010).

[74] G. Radel and R. Beyer, Neutrino electron scattering, Mod. Phys. Lett. A **08,** 1067 (1993).

[75] M. Lindner, F. S. Queiroz, W. Rodejohann, and X.-J. Xu, Neutrino-electron scattering: General constraints on Z' and dark photon models, J. High Energy Phys. 05 (2018) 098.

[76] M. Abdullah, J. B. Dent, B. Dutta, G. L. Kane, S. Liao, and L. E. Strigari, Coherent elastic neutrino nucleus scattering (CEνNS) as a probe of Z' through kinetic and mass mixing effects, Phys. Rev. D **98,** 015005 (2018).

[77] F. J. Hasert *et al.*, Search for elastic ν_μ electron scattering, Phys. Lett. **46B,** 121 (1973).

[78] M. Williams, C. P. Burgess, A. Maharana, and F. Quevedo, New constraints (and motivations) for Abelian gauge bosons in the MeV-TeV mass range, J. High Energy Phys. 08 (2011) 106.

[79] C. Patrignani *et al.* (Particle Data Group Collaboration), Review of particle physics, Chin. Phys. C **40,** 100001 (2016).

[80] M. Czakon, J. Gluza, F. Jegerlehner, and M. Zralek, Confronting electroweak precision measurements with new physics models, Eur. Phys. J. C **13,** 275 (2000).

[81] A. M. Sirunyan *et al.* (CMS Collaboration), Search for high-mass resonances in dilepton final states in proton-proton

collisions at $\sqrt{s} = 13$ TeV, J. High Energy Phys. 06 (2018) 120.

[82] A. Gulov, A. Pankov, A. Pevzner, and V. Skalozub, Model-independent constraints on the Abelian Z' couplings within the ATLAS data on the dilepton production processes at $\sqrt{s} = 13$ TeV, Nonlinear Phenom. Complex Syst. **21**, 21 (2018).

[83] A. Pevzner, Influence of the Z-Z' mixing on the Z' production cross section in the model-independent approach, Nonlinear Phenom. Complex Syst. **21**, 30 (2018).

[84] R. Hamberg, W. L. van Neerven, and T. Matsuura, A complete calculation of the order $\alpha - s^2$ correction to the Drell-Yan K factor, Nucl. Phys. **B359**, 343 (1991); Erratum **B644**, 403(E) (2002).